

PCCP

Accepted Manuscript



This is an *Accepted Manuscript*, which has been through the Royal Society of Chemistry peer review process and has been accepted for publication.

Accepted Manuscripts are published online shortly after acceptance, before technical editing, formatting and proof reading. Using this free service, authors can make their results available to the community, in citable form, before we publish the edited article. We will replace this *Accepted Manuscript* with the edited and formatted *Advance Article* as soon as it is available.

You can find more information about *Accepted Manuscripts* in the [Information for Authors](#).

Please note that technical editing may introduce minor changes to the text and/or graphics, which may alter content. The journal's standard [Terms & Conditions](#) and the [Ethical guidelines](#) still apply. In no event shall the Royal Society of Chemistry be held responsible for any errors or omissions in this *Accepted Manuscript* or any consequences arising from the use of any information it contains.

The reactivity game: Theoretical predictions for heavy atom tunneling on adamantyl and related carbenes

Cite this: DOI: 10.1039/x0xx00000x

S. Kozuch^a

Received 00th January 2012,
Accepted 00th January 2012

DOI: 10.1039/x0xx00000x

www.rsc.org/

The possibility of carbon atom tunneling at cryogenic temperatures for carbene-based ring expansion of adamantane analogues calls for a delicate balance of reactivity to experimentally detect the transpiring reaction. An overly reactive carbene will precipitously decay; an excessively stable carbene will not tunnel. Nevertheless, the factors that affect the quantum-mechanical tunneling (QMT) reactivity–mass, barrier height and width– are strikingly different from the classical “over the barrier” thermal mechanism. Herein, comparisons with experimental values and predictions on measurable rate constants for novel carbene systems are presented by way of small curvature tunneling (SCT) computations. Adamantane, noradamantane and bisnoradamantane have a significantly different C-C bond strain and reactivity, which can be modulated by tinkering with the carbene substituent atom (H, Cl or F) to obtain an observable lifetime of the reactant. The influence of barrier heights and widths, kinetic isotope effects (KIE), the detection of the tunneling-determining atoms (TDA) and the comparisons with hydrogen-based reactions are discussed with the objective of finding the physical limits for QMT.

Introduction

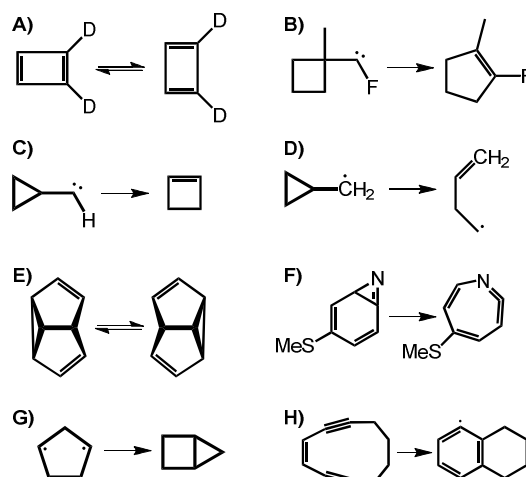
Quantum-mechanical tunneling (QMT) is a well-known mechanism for reactions involving the displacement of hydrogen atoms.¹ The tunneling probability is increased by a small mass of the moving parts of the molecule, thus the light H atom allows an easy non-classical pathway. This QMT probability decreases as the exponential of the square root of the shifting mass and barrier height (ΔE^\ddagger). However, the probability is directly proportional to the exponential of the negative of the barrier width (a variable that has no importance on transition state theory), making the amplitude of the atomic movements the most critical factor for a swift tunneling.^{1–3} This trend can be

$$P \propto e^{-x w \sqrt{\Delta E^\ddagger m}} \quad (1)$$

where P is the tunneling probability, w is the width of the barrier, ΔE^\ddagger the activation energy, m the mass of the moving parts, and x a factor that depends on the shape of the potential energy curve (for a rectangular barrier, $x = 2\sqrt{2}/\hbar$).¹

Whitman and Carpenter^{4–6} proved that the bond shifting (a.k.a. automerization) of cyclobutadiene-1,4-d₂ proceeds by QMT, thus showing the first example of a “heavy” atom tunneling. In the last decade, several other reactions of this nature have been observed and/or computed (see Scheme 1), all of them sharing the same characteristics: a rather low ΔE^\ddagger (but not too low, in

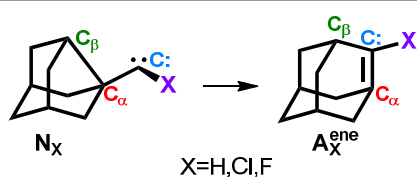
such a way that it can be distinguished from a thermally activated classical mechanisms), and a narrow barrier on the reaction coordinate.



Scheme 1 Some observed or computed reactions taking place by heavy atom tunneling. A) Cyclobutadiene automerization.^{4–6} B) Methyl-cyclobutyl-fluorocarbene ring expansion.⁷ C) Cyclopropyl-carbene ring expansion.⁸ D) Ring opening of cyclopropyl-carbinyl radical.^{9,10} E) Degenerate rearrangement of semibullvalene.¹¹ F) Ketenimine ring expansion.¹² G) Ring closure of cyclopentane-1,3-diyli.^{13,14} H) Bergman cyclization of a 10-membered-ring enediyne.¹⁵ Reactions (A) to (G) occur at cryogenic conditions from the ground vibrationally state.

Carbenes from adamantane analogues

Another reaction studied experimentally¹⁶ and theoretically¹⁷ was the ring expansion of Noradamantyl-carbenes (N_X , with $X = H, Me, Cl$ or F , see Scheme 2) to form substituted Adamantenes (A_X^{ene}).



Scheme 2 Ring expansion of Noradamantyl-carbenes^{16,17} forming Adamantenes.

The Noradamantane skeleton has a strained σ C-C bond (0.12 Å longer than the other two bonds adjacent to the carbene in N_{Cl}) that can hyperconjugate with the empty p atomic orbital (AO) of the carbene (see Fig. 1A). Accordingly, the most stable conformer has a small $C:-C_{\alpha}-C_{\beta}$ angle (only 100° in N_{Cl}), and an almost perpendicular $C_{\beta}-C_{\alpha}-C:-Cl$ dihedral angle (97° , see Fig. 2). This geometry is close to the transition state for the ring opening, and therefore the atoms must only shift a short distance to break the $C_{\alpha}-C_{\beta}$ and form the $C:-C_{\beta}$ bonds. In addition, the reactivity of this system produces a strongly exothermic reaction (see Table 1), a factor that further narrows the barrier. As a result, these carbenes attached to strained cycles (usually produced by photolysis of a diazirine compound¹⁸) are excellent candidates for heavy atom tunneling (similar to the reactions of Schemes 1B and 1C).

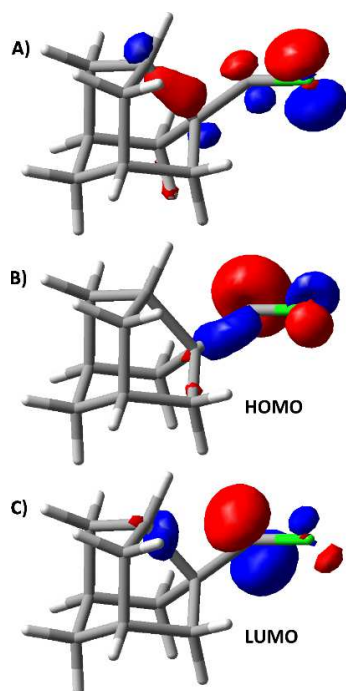


Figure 1 (A) Low lying molecular orbital showing the charge transfer (hyperconjugation) of the strained $C_{\alpha}-C_{\beta}$ σ bond and of the Cl p AO towards the empty p AO on the carbene of N_{Cl} . (B) The HOMO, mostly localized in the sp hybrid orbital ("lone pair") of the carbene. (C) The LUMO, primarily on the p AO of the carbene.

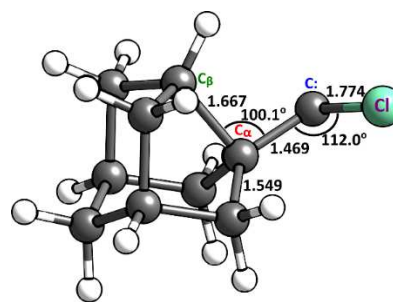


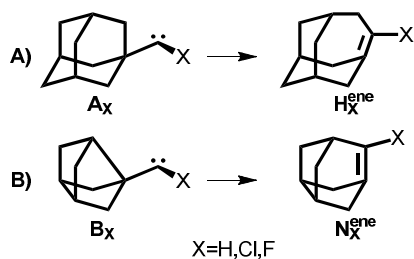
Figure 2 Most stable conformer of N_{Cl} , with selected bond distances (in Å) and angles. The dihedral angle between the Cl and the strained C-C bond ($C_{\beta}-C_{\alpha}-C:-Cl$) is 97.2° (geometry taken from ref. 17).

The stabilization of the carbene awarded by the substituent atom provides the first dimension for the reactivity towards the ring expansion. The fluoride in N_F stabilizes the carbene by $p \rightarrow p$ electron donation (see Fig. 1A) more than the chloride in N_{Cl} .¹⁹ Consequently, N_F has a higher activation barrier[†] than N_{Cl} (9.7 vs. 5.8 kcal/mol) making the tunneling at cryogenic conditions of N_F probably too slow to be observed experimentally (with a calculated half-life of millions of years).^{16,17} The ring expansion of methyl-cyclobutyl-fluorocarbene (Scheme 1B), thanks to the stressed four-carbon ring, actually requires the "decelerating" effect of the F substituent to make the reaction experimentally observable.

In contrast to the stability provided by the halides, a simple hydrogen substituent (as in N_H) produces a severely reactive carbene, due to the lack of p electrons on H to donate.^{19,20} The cyclopropyl-carbene ring expansion shown in Scheme 1C is an example where the relative stability of the ring requires an H substituent on the carbene to "accelerate" the reaction in order to occur at cryogenic temperature.⁸ The calculated reaction barrier for the ring expansion of N_H is negligible (0.5 kcal/mol), and the reaction is virtually instantaneous at any temperature,^{16,20,21} making it impossible to distinguish between the classical and QMT mechanisms.

The second dimension of the reactivity resides in the tension on the $C_{\alpha}-C_{\beta}$ bond. Adamantane does not have a strained bond as the one in noradamantane, and therefore an adamantyl-carbene (A_X , see Scheme 3A) will be less reactive compared to a noradamantyl-carbene. Indeed, A_{Cl} is stable at low temperature.²² Furthermore, A_H can be chemically trapped by solvent molecules or scavengers before the ring expansion can occur, while the much more reactive N_H falls directly to the adamantene product before being trapped (still, A_H was never detected in an argon matrix, suggesting a faster tunneling than N_{Cl}).²⁰ All this indicates a much longer lifetime for adamantyl-compared to noradamantyl-carbenes.

In contrast to the stable bonds in the adamantane structure, bisnoradamantane has two strained C-C bonds acting in a synergetic manner, making it even more reactive than noradamantane. Therefore, bisnoradamantyl-carbene systems (B_X , Scheme 3B) should react extremely fast towards the ring-expansion.



Scheme 3 Ring expansion of (A) adamantyl-carbene (A_x) to form a homoadamantene (H_x^{ene}), and (B) bisnoradamantyl-carbene (B_x) to form a noradamantene (N_x^{ene}).

As a measure of the reactivity of the three described moieties (adamantane < noradamantane < bisnoradamantane), the exothermicity towards the hydrogenolysis of the strained bonds was calculated (in the case of adamantane all bonds are equivalent), resulting in a clear trend of -10.6, -26.0 and -51.7 kcal/mol, respectively. Another measure of the C-C bond strain is the C-C bond length; taking as a reference the stable bonds of adamantane (1.544 Å), the strained bond of bisnoradamantane is longer by 5.2 %, and of noradamantane by 3.3 % (with the rest of the C-C bonds ranging from 0.7 % longer to 0.2 % shorter, see geometries in the ESI). Evidently there is a ladder of reactivity going from adamantane to noradamantane to bisnoradamantane, parallel to the reactivity going from hydro to chloro to fluoro-carbenes, as depicted in Table 1.

Table 1 Energies of activation^a and of reaction for the ring expansion of adamantyl, noradamantyl and bisnoradamantyl carbenes (see Schemes 2 and 3), in kcal/mol calculated at the B3LYP/6-31G(d) level.

X=	A_x			N_x			B_x		
	H ^a	Cl	F	H ^a	Cl ^b	F ^b	H	Cl	F
ΔE^\ddagger	6.2	15.3	19.1	0.5	5.8	9.7	No barrier	2.3	5.7
ΔE_{rx}	-47.8	-31.3	-29.7	-33.9	-21.5	-21.0		-32.5	-32.7

^a See also Ref. 20.

^b See also Refs. 16 and 17.

In this work, and following a previous communication,¹⁷ the question of finding the right combination of reactivity that can produce an experimentally observable lifetime window for the ring expansion by carbenes through heavy atom quantum tunneling was tackled. In addition, a rationalisation of the experimental outcomes of some of these systems was pursued,^{16,20} and the possibility of having tunneling controlled^{18,23,24} hydrogen shifts as competing reactions was considered. When dealing with quantum tunneling this is not just a matter of finding the right barrier height (Table 1) since, as explained before (eq. 1), we must take into account also the displaced masses and, most critically, the width of the barriers. Therefore, a comparison of the requirements for hydrogen and carbon QMT was carried out.

Theoretical Method

There are several semi-quantitative methods to estimate the tunneling correction to the rate constant, including the renowned Wigner correction (it must be noted that this correction fails at low temperatures, see ESI).¹ However, these methods do not mimic the real shape of the reaction coordinate, nor take into account the possibility of “cutting corners” of the reaction coordinate to pass through the least-action pathway.²⁵ A considerably more accurate (and significantly more demanding) method for reactions whose least-action pathway lies close to the reaction coordinate is the small-curvature tunneling (SCT) approximation,²⁶ which was the one used in this and previous¹⁷ works. This method remedies the deficiencies of Wigner and other corrections by “plotting” the potential energy surface surrounding the valley of minimum energy. To this end, it calculates energies, energy gradients and second derivatives, not only at the reactant and TS geometries but also at many points along the reaction pathway.

Because of the massive computational cost of the SCT calculation, it cannot be carried out with a high quality ab initio method. We employed for this purpose the B3LYP functional^{27,28} with a very small basis set, 6-31G(d),²⁹ except for the H-shift reactions calculated with 6-31G(d,p), a more accurate basis set when a hydrogen is the central atom of the reaction (when the migrating atom is not an H, the difference between both basis sets is negligible).¹⁷ Admittedly, this is hardly the best method for most barrier calculations.³⁰ However, previous comparisons to CCSD(T) benchmarks¹⁷ and experimentally obtained rate constant¹⁶ proved that for these specific carbene reactions it is actually a very reliable methodology.

All DFT electronic structure calculations were performed with Gaussian09.³¹ The rate constant calculations were done with Polyrate,³² using Gaussrate³³ as the interface between Polyrate and Gaussian09. Classical rate constants were computed using canonical variational transition state theory (CVT),³⁴ and SCT was used for the tunneling correction,²⁶ with a step size of 0.001 Bohr and quantized reactant state tunneling (QRST)³⁵ for the reaction coordinate mode. Unless specified, SCT rate constant values will include the CVT component.

Results and Discussion

Table 2 shows the rate constants with and without tunneling corrections (SCT and CVT, respectively), at cryogenic temperature (10 K) and close to room temperature (300 K). The full tables at a wide range of temperatures can be found in the ESI. In all cases, SCT rates are several orders of magnitude faster than raw CVT values at very low T. This is not unexpected, since the thermal energy required to pass over the reaction barrier is virtually inexistent in these conditions (except for N_H and B_H , having negligible or null barriers, see table 1). However, the fact that tunneling is significantly more probable than classical reactivity is not enough to indicate that the reaction can proceed at experimentally measurable times, as shown in the calculated half-lives of table 2.

Table 2. Classical (CVT) and tunneling corrected (SCT) rate constants in s^{-1} at 10 K and 300 K, and the half-life of the reactants for the ring expansion reaction (in hours, including tunneling).

X=		A_x			N_x			B_x		
		H	Cl	F	H	Cl ^a	F ^a	H	Cl	F
10 K	CVT	1.5×10^{-125}	5.8×10^{-307}	2.0×10^{-390}	8.7×10^2	7.8×10^{-103}	1.6×10^{-190}	No Barrier	4.7×10^{-29}	1.0×10^{-99}
	SCT	6.8×10^{-4}	2.7×10^{-31}	3.6×10^{-35}	2.8×10^{11}	3.7×10^{-7}	7.3×10^{-16}		5.6×10^2	4.8×10^{-7}
	$t_{1/2}$	2.8×10^{-1}	7.2×10^{26}	5.3×10^{30}	7.0×10^{-16}	5.1×10^2	2.6×10^{11}		3.4×10^{-7}	4.0×10^2
300 K	CVT	1.3×10^8	4.4×10^1	6.5×10^{-2}	3.4×10^{12}	3.1×10^8	3.8×10^5		1.0×10^{11}	3.3×10^8
	SCT	1.4×10^8	5.5×10^1	8.4×10^{-2}	3.3×10^{12}	3.6×10^8	4.3×10^5		1.1×10^{11}	3.7×10^8
	$t_{1/2}$	1.4×10^{-12}	3.5×10^{-6}	2.3×10^{-3}	5.8×10^{-17}	5.4×10^{-13}	4.5×10^{-10}		1.7×10^{-15}	5.3×10^{-13}

^a From ref. 17.

A_{Cl} , A_F and N_F will show virtually no ring expansion products (in a reasonable time). Inversely, the abrupt reactions on N_H , B_{Cl} and B_H will probably make impossible the detection of the carbene reactants and to measure their rate constant. These differences in reactivity are not only caused by the height of the barriers, and certainly not by the mass of the H, Cl or F substituents (which are not significantly moving, see later Figs. 5 and 6); the main factor resides in the width of the barrier (see eq. 1).

Figure 3 shows for the noradamantyl-carbenes the displacement of the carbene (the tunneling-determining atom –TDA– for these molecules, see later Fig. 5) from the reactant until the reaction starts to be exergonic (crossing the zero Gibbs energy line). It is clear that the lower the barrier, the narrower it tends to be. This can be seen as a corollary of Hammond's postulate, pointing to a tighter barrier when having an early transition state resembling the reactant. Still, as we shall see later, this is only an approximate feature, and small differences in the barrier width may have a great impact on the rate.

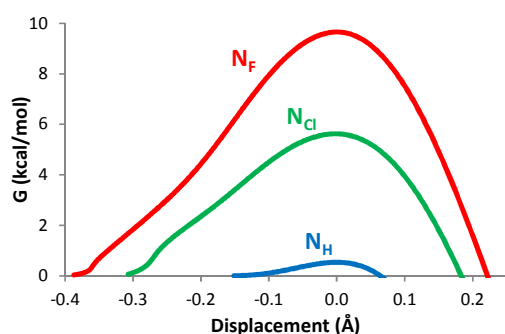


Figure 3 Gibbs energy vs. C: atom displacement in the ring-expansion reaction for N_H , N_{Cl} and N_F . Zero displacement corresponds to the transition state geometry.

Figure 4 shows an Arrhenius graph for the three “observable” systems, A_H , N_{Cl} and B_F . The tunneling corrected curves depart from the CVT values at $T \lesssim 100$ K. A plateau for the rate constants at increasingly low temperatures indicates that the tunneling proceeds mostly from the ground vibrational level. The threshold temperature for this plateau is ~ 50 K for A_H , and ~ 20

K for N_{Cl} and B_F . Above these temperatures, QMT from the vibrationally excited states have the lion's share of the process; their population is still low compared to the ground state, but their higher energy makes the effective barrier lower and narrower, and consequently the tunneling more probable. At approximately 150 K the three systems begin to behave classically, with the CVT rates being higher than the tunneling correction.

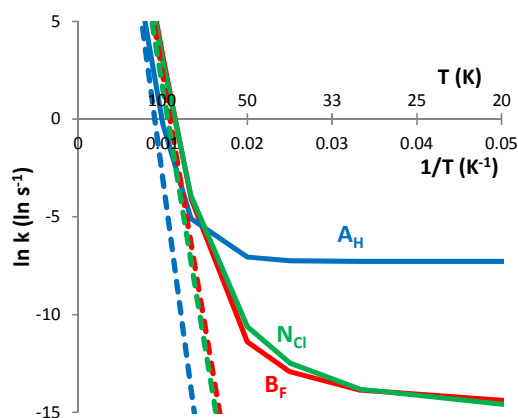


Figure 4 Arrhenius graph for the ring expansion reaction of A_H , N_{Cl} and B_F . Dotted lines corresponds to the CVT (classical) rate constants, while continuous lines are SCT (classical + tunneling) values.

N_{Cl} and B_F have a practically identical rate profile both at low and high temperatures, with A_H as the odd one out of this triad. At high temperature (classical regime) the ring expansion rate of reaction of A_H is very similar to the other two systems, as would be expected from their similar ΔE^\ddagger . But when approaching the absolute zero, A_H generates a more than three orders of magnitude faster reaction.

The experimental rate of reaction for N_{Cl} was measured by Moss et. al., with a value of $k \approx 2.3 \times 10^{-7} s^{-1}$ at 9 K in an argon matrix,¹⁶ remarkably close to the one calculated by SCT, $3.7 \times 10^{-7} s^{-1}$.¹⁷ This gives the confidence to predict that B_F will also be observed to tunnel at similar times, if the bisnoradamantyl-carbene can be synthesized.

\mathbf{A}_H was not observed experimentally at low T, but as explained before, its stability was long enough to be trapped by scavengers at 15 °C (opposed to \mathbf{N}_H , that readily falls to adamantene).²⁰ The lifetime of \mathbf{A}_H was estimated in the order of the nanoseconds at 300 K, in fair agreement with classical TST calculations. In an argon matrix at 14 K the $\mathbf{H}_H^{\text{ene}}$ product was directly observed after irradiation of the diazirine precursor, without IR evidence of a stable carbene (a clear sign of a fast heavy atom tunneling). According to the SCT calculations (Table 2), the lifetime of \mathbf{A}_H is 2000 times faster than \mathbf{N}_{Cl} , implying that if the adamantyl-carbene is to be experimentally observed, the IR spectrum should be recorded only minutes after the photolysis.⁸

The question that begs to be answer is: Why \mathbf{A}_H is much more reactive than \mathbf{N}_{Cl} and \mathbf{B}_F at low temperatures, even when it is more than two times slower at room temperature?

Kinetic isotope effects (KIE) and atomic displacements

In hydrogen-based reactions it is presumed that the sole atom that tunnels is the light hydrogen; given that the reduced mass is the factor to take into account,¹ this is usually a valid approximation. However, in reactions including heavy atom tunneling, the reduced mass is a complex combination of the different moving parts of the system. To understand the influence of these parts on the ring expansion and detect the tunneling-determining atom (TDA), several KIE calculations were performed, and the displacement of the critical atoms was analyzed (see Figs. 5, 6 and 7).

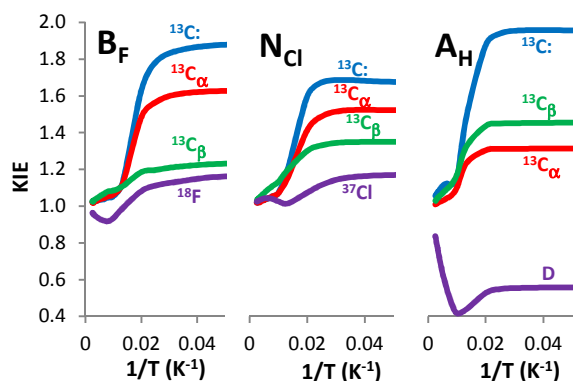


Figure 5 Kinetic Isotope Effect (KIE) in the ring expansion reactions for the carbene (\mathbf{C}), the α and β carbons, and the heteroatom (^{18}F , ^{37}Cl and D) in \mathbf{B}_F , \mathbf{N}_{Cl} and \mathbf{A}_H .

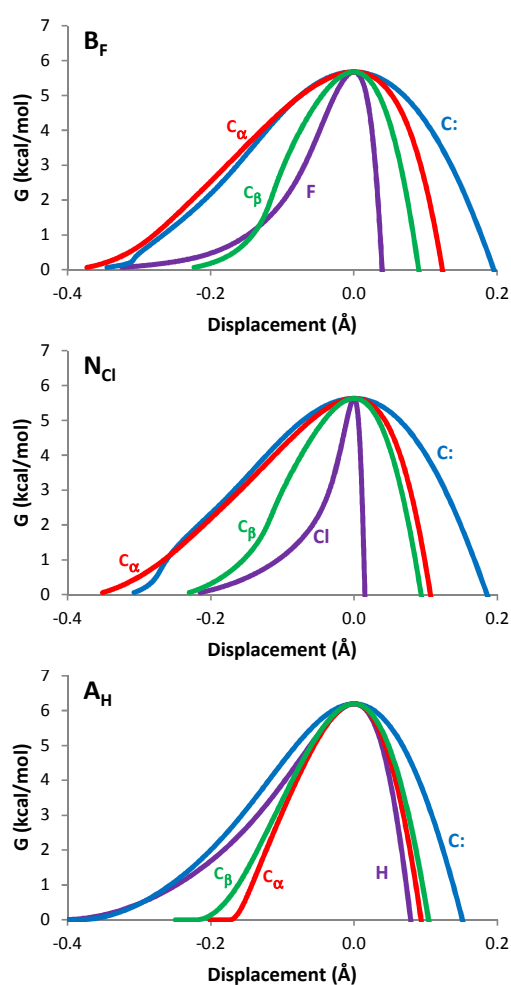


Figure 6 Atomic displacements in the ring expansion reaction for the carbene, the α and β carbons, and the heteroatom (F, Cl and H) in \mathbf{B}_F , \mathbf{N}_{Cl} and \mathbf{A}_H .

By comparing the KIEs (Fig. 5) to the atomic displacements (Fig. 6), it is possible to see their relation: the wider the trajectory of an atom, the higher its KIE for a QMT mechanism.

The three carbons (\mathbf{C} , \mathbf{C}_α and \mathbf{C}_β) show similar displacements along the reaction coordinate. However, in the three examined reactants (\mathbf{A}_H , \mathbf{N}_{Cl} and \mathbf{B}_F) the carbene atom is the one that has a wider trajectory, and consequently is the TDA. The KIE of \mathbf{C} : (measured as $^{12}\text{K}/^{13}\text{K}$) is the highest on each system, reaching values of 2.0, 1.7 and 1.9 at cryogenic conditions for \mathbf{A}_H , \mathbf{N}_{Cl} and \mathbf{B}_F (compare to the “standard” values of 1.08, 1.03 and 1.03, respectively, at 300 K, where tunneling is negligible). The other two carbons have a smaller but still appreciable effect on the rate of reaction. For \mathbf{B}_F and \mathbf{N}_{Cl} the α carbon is the second in importance, moving away as the strain of the C-C bond is released in the ring expansion. In \mathbf{A}_H the β carbon has a wider trajectory compared to the α one, and a resulting higher KIE.

The Cl and F substituents have considerable KIE values (1.17 and 1.18 at low T), but they are much less significant than the KIE of the previously described carbons. The displacement of Cl and F in \mathbf{N}_{Cl} and \mathbf{B}_F is small, especially approaching the transition state (see Figs. 6 and 7). At that point, where the energy is a maximum, the extent of the displacement is more important

than closer to the reactant, where the energy profile is much lower and the tunneling easier. This is decisive for heavier atoms, especially for the “massive” chlorine. The importance of the reaction coordinate width at the TS is the reason why the Wigner approximation only requires as input the magnitude of the imaginary frequency.¹ Although the different isotopic relations ($^{12}\text{C}_k/^{13}\text{C}_k$, $^{18}\text{F}_k/^{19}\text{F}_k$, and $^{35}\text{Cl}_k/^{37}\text{Cl}_k$) make it difficult to draw quantitative conclusions, we can say that the weight of the halides does not significantly affect the tunneling rates (although their electronic effects do).

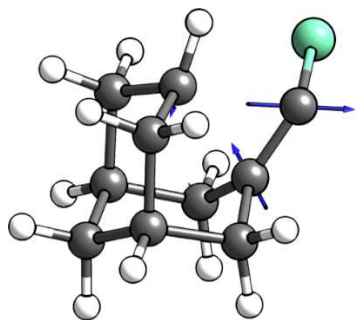


Figure 7 Scaled vectors for the heavy atom displacements at the TS of the ring expansion for \mathbf{N}_G . The carbene atom has the broadest trajectory at this point, followed by the α carbon (moving in the opposite direction), and finally by the β carbon. The chlorine is almost static close to the TS.

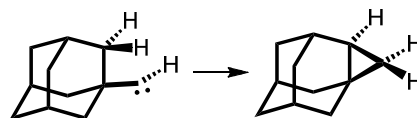
The deuterium kinetic isotope effect in \mathbf{A}_H is extremely small (0.56 at 10 K), caused by a classical inverted secondary KIE. The tunneling effect starts to reverse this trend below ~ 100 K (with a minimum $^{\text{H}}k/^{\text{D}}k = 0.42$), and flattens at $T < 50$ K. In other words, a small substituent atom mass helps the tunneling mechanism, but it cannot compensate the inverse effect on the zero-point energy that acts at higher temperatures and favours higher masses. On a more thorough observation of the fluoride KIE in \mathbf{B}_F (Fig. 5), we can see that the same trend occurs for this heavier substituent, although in this case the tunneling easily overcomes the inverted KIE.

The study of the KIE gives information on relative rate constants, but it does not reveal absolute rates, and it does not answer the question of the fast ring expansion of \mathbf{A}_H . However, a visual analysis of the displacement graphs (Fig. 6) reveals that the amplitude of the trajectory of the determining atom ($\mathbf{C}:$) is shorter in \mathbf{A}_H than in \mathbf{N}_{Cl} and \mathbf{B}_F . If we take as a qualitative measure the amplitude of the carbene atom displacement at half-barrier height, it moves 0.26 \AA in \mathbf{A}_H , and 0.31 \AA in \mathbf{N}_{Cl} and \mathbf{B}_F . Since the tunneling probability depends exponentially on the width, the difference of 0.05 \AA can account for the three orders of magnitude faster ring opening, even when the barriers are of similar heights. The imaginary frequencies of the transition states also hints to a tighter barrier through a stronger curvature at the energy peaks, with 430 cm^{-1} for \mathbf{A}_H , 338 cm^{-1} for \mathbf{N}_{Cl} and 299 cm^{-1} for \mathbf{B}_F . Therefore, the requirement of a narrow reaction pathway to observe a QMT event is taken to an extreme in \mathbf{A}_H , where it has such an ephemeral existence that it will be very hard to observe before falling to the product.²⁰

H-migration by tunneling control?

Several contingencies may hinder the observation of the ring expansion products. For instance, in methyl-noradamantyl-carbene (\mathbf{N}_{Me}) it has been calculated and predicted that even though there is a higher activation energy for a 1,2-hydrogen-shift from the Me group to form a vinyl product compared to the ring expansion, at cryogenic conditions the H-shift is actually favored.¹⁷ This effect was termed “tunneling control”,^{8,23,24,36} when owing to the characteristics of the reaction (in this case the small mass of the shifting H) the reaction outcome will be different to the kinetically or thermodynamically controlled cases.

In the systems studied here there is no methyl group bonded to the carbene, but the close by hydrogens on the β carbon might shift and generate a cyclopropyl ring, especially in the adamantyl case, as depicted in Scheme 4.



Scheme 4 Hypothetical formation of a cyclopropyl ring by 1,3-hydrogen shift on \mathbf{A}_H .

This reaction has a ΔE^\ddagger of 19.2 kcal/mol , significantly higher than the 6.2 kcal/mol for the ring expansion of \mathbf{A}_H ; but again, in the H-shift the displaced mass is significantly lighter than carbons of the ring expansion. Nevertheless, SCT calculations conclude that in this case there is no tunneling control, and the H-shift reaction is 9 orders of magnitude slower than ring expansion at low temperatures ($k = 7.8 \times 10^{-13} \text{ s}^{-1}$ at 10 K). To the best of our knowledge, and agreeing with the above result, this reaction has not been observed experimentally.

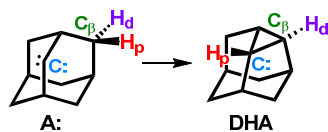
The fast hydrogen migration in the \mathbf{N}_{Me} case¹⁷ has two advantages with respect to our \mathbf{A}_H system. First, the ΔE^\ddagger is lower by 9.4 kcal/mol ; but more important, in the former case we have a 1,2-H-shift, while in the later it is a 1,3-H-shift, making it a wider barrier.

Near room temperature (300 K) the ring opening is still 8 orders of magnitude faster than the H-shift in \mathbf{A}_H . However, there is a significant weight of vibrationally activated tunneling for the hydrogen migration, making the SCT rate constant 5 times faster than the purely classical CVT value (1.8 vs. 0.35 s^{-1}), while in the ring expansion there is virtually no tunneling involved (see table 2). This indicates that for systems where H-shifting is the main reaction, QMT should not be disregarded from the rate constant calculation even at room temperature.

Adamantylidene, a limit case for hydrogen tunneling

Still working in the adamantane analogues business, one reaction that may provide the limits of hydrogen QMT is the 1,3-H-shift of adamantylidene ($\mathbf{A}:$) to form 2,4-dehydroadamantane (\mathbf{DHA}), as depicted in Scheme 5 (the 1,2-H-shift is hindered by geometrical constraints³⁷). The reaction can also be considered a cyclopropanation, since after the migration of the proximal hydrogen (\mathbf{H}_p) an ephemeral singlet diradical is formed (actually,

an unstable inflection point in the potential energy surface), which promptly creates the covalent bond between the former carbene ($C:$) and the beta to the carbene carbon atom (C_{β}) in a concerted mechanism.



Scheme 5 Formation of 2,4-dehydroadamantane from adamantylidene after a concerted 1,3-H-shift and cyclopropanation.

The reaction is known since 1966, when it was first reported by Udding and coworkers.³⁸ Since the carbene was formed by pyrolysis of a tosylhydrazone salt, there was no way to measure the rate of reaction at low temperatures. In a much later study in which the reaction was initiated by photolysis, it was observed that in an argon matrix at 10 K the carbene was stable, producing **DHA** by further irradiation;³⁷ however, the lifetime and natural decay of **A:** in these conditions was not measured. Still, in a cyclodextrin host at 77 K the formation of **DHA** was observed (along other intermolecular parallel reactions).³⁹

A simple calculation at the B3LYP/6-31G(d,p) level provides a ΔE^{\ddagger} of 11.6 kcal/mol, and $\Delta G^{\ddagger} = 10.8$ kcal/mol (see also Ref. 40). A classical CVT calculation gives a rate of reaction of $1.5 \times 10^{-18} \text{ s}^{-1}$ at 77 K for this reaction, with a half-life of roughly the currently accepted age of the universe. Therefore, QMT of the migrating H would be the sensible mechanism.

The rate constant including tunneling correction (SCT) gives a value of $k = 3.0 \times 10^{-6} \text{ s}^{-1}$ at 10 K (tunneling from the ground vibrational state), $9.3 \times 10^{-6} \text{ s}^{-1}$ at 77 K (including tunneling from vibrationally excited states), and $1.4 \times 10^5 \text{ s}^{-1}$ at 300 K (approximately twice the CVT value). Therefore, these calculations predict that up to room temperature most of this 1,3-H-shift occur by QMT, and at cryogenic temperatures the half-life of **A:** will be only an order of magnitude shorter than the $t_{1/2}$ of **NCl** or **BF** (64 hours). Adamantylidene should be experimentally detectable in these conditions for several days, while **DHA** is slowly formed.

Adamantylidene deviates from a high C_{2v} geometry because of a hyperconjugation effect with the vicinal C-C σ bonds, which can explain the relative stability of this molecule.^{40,41} This hyperconjugation causes the carbene atom to slightly tilt to one side (resulting in a C_s symmetry), giving the proximal H a higher probability to migrate. The TS of the H-shift reaction is presented in Fig. 8, including the most important displacement vectors along the reaction coordinate.

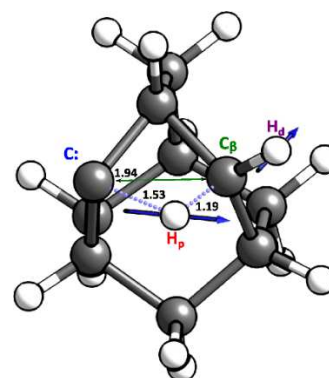


Figure 8 Transition state geometry of the **A:** \rightarrow **DHA** reaction, including some critical bond distances and the scaled displacement vectors.

From Fig. 8 it can be deduced that H_p has the wider displacement, while the distal hydrogen (H_d) moves to stabilize a momentary planar conformation on C_{β} , corresponding to an unstable radical. This is a very early TS, quite far from the product geometry. Once again, the high exothermicity of the reaction ($\Delta E_{rx} = -58.3$ kcal/mol) plays in favor of the tunneling mechanism by narrowing the barrier.

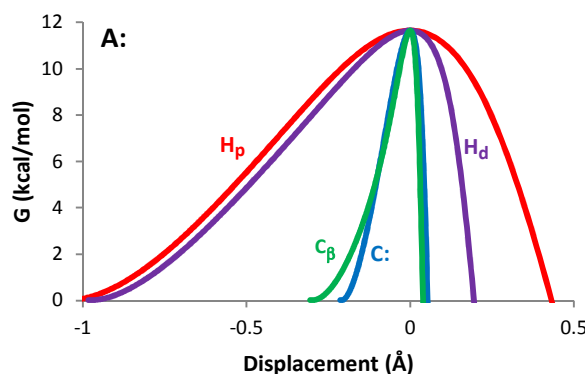


Figure 9 Displacement vs. free energy of the critical atoms for **A:** \rightarrow **DHA** (see Scheme 5).

Fig. 9 shows the displacement of the four specified atoms. There is no doubt that the carbons are mostly static compared to the hydrogens. The half-height barrier widths are 0.78, 0.58, 0.13 and 0.12 Å for H_p , H_d , $C:$ and C_{β} , respectively. This might indicate that the small movement of the carbon can affect the kinetics, but probably in a much lesser extent than in the ring-expansion reactions. Since the SCT approximation does not necessarily follow to the letter the path of minimum energy, but the path of minimum action²⁵ (as long as it is close to the former), the influence of each atom should be properly gauged by a kinetic isotope effect calculation.

The KIE values ($^1H_k/^2D_k$ and $^{12}C_k/^{13}C_k$) at room temperatures are 2.44, 1.54, 1.01 and 1.05 for H_p , H_d , $C:$ and C_{β} , respectively. These are ordinary semi-classical values, and even the value for H_p may be considered small for a first order KIE involving a migrating H. However, as we move to cryogenic conditions, the picture gets radically different. At 10 K $C:$ has a KIE of 1.21, and C_{β} of 1.37, implying at best a moderate influence of the

carbons on the tunneling, corresponding to their very short displacement. Substituting the hydrogens for deuteriums has a much more drastic effect. **H_d** has a KIE of 65, and **H_p** of 5863. In this tunneling process, the proximal hydrogen is “guilty as charged” and, not surprisingly, it is the TDA.

Tunneling limits

Since the H-shift of **A:** and the ring expansions of **N_{Cl}** and **B_F** have similar tunneling rates, which are not far from the measurable limits in a normal experimental project, this can serve us to compare the minimum requirements to observe carbon and hydrogen tunneling. The height and half-height width of the TDA in the barriers for **N_{Cl}** and **B_F** ring expansions are circa 6 kcal/mol and 0.3 Å, whereas for **A:** H-shift they are 12 kcal/mol and 0.8 Å. It can be deduced that, as a very rough rule of thumb, these values mark the limits of quantifiable kinetics by QMT from the ground state: carbon atom tunneling will be possible with barriers half the height and three times slimmer than the maximum barriers for H tunneling. This has sense if we recall the introductory claim that the probability of tunneling decreases with the power of the barrier width times the square root of the barrier height and mass (eq. 1).¹ Mathematically, we can express this as:

$$P \propto e^{-x w_H \sqrt{\Delta E_H^\ddagger m_H}} \approx e^{-x w_C \sqrt{\Delta E_C^\ddagger m_C}} \quad (2)$$

where now we are defining w as the half-height width of the barrier, and m is the mass of the TDA for the H or C shifting reactions. As $m_C = 12 m_H$, we can derive that if $\Delta E_H^\ddagger \approx 2 \Delta E_C^\ddagger$, then w_C will be approximately a third of w_H , close to the previous comparison of the H-shift of **A:** and the ring-expansion of **N_{Cl}** or **B_F**.

Considering the tunneling rates of all our systems, we might venture (again, as a rough rule of thumb) to express a “tunneling limit” (T_L) as

$$T_L = w \sqrt{\Delta E^\ddagger m} \quad (3)$$

where again w is the half-height width of the barrier, and m is the mass of the TDA. Low T_L should correlate with a high tunneling probability and short lifetime of the reactant. QMT reactions with T_L close to 2.6 (as **N_{Cl}** and **B_F** ring expansions, and **A:** hydrogen shift, see Table 3) will have the right lifetime window to be observed at cryogenic temperatures. With a T_L over 2.6 we are crossing the limit of tunneling from the ground state. T_L has an approximately linear tendency vis-à-vis $\ln k$ for all the reactions studied in this paper (see fig. 10). Therefore, the use of the $T_L \approx 2.6$ limit may be a fast and easy method for a qualitative screening of systems driven by QMT at cryogenic temperatures. This only requires the calculation of the intrinsic-reaction coordinate. The validity of this rule will be analyzed for different systems in subsequent studies.

(Disclaimer: this T_L boundary may be affected by reactions without a clear TDA, by the formation of unexpected compounds or inefficient quenching,⁸ by systems where the least action

pathway lies far from the minimum energy path, or any other unforeseen condition. The author is not responsible for the use or misuse of T_L by a third party.)

Table 3 Activation energies, barrier widths, mass of the tunneling-determining atom (in kcal/mol, Å and atomic mass units, respectively), tunneling limit (eq. 3) and natural logarithm of the SCT rate constant at 10 K for all the reactions studied here.

X=	A _x			N _x			B _x		A: A _H	
	H	Cl	F	H	Cl	F	Cl	F	(1,3-H-shift)	
ΔE^\ddagger	6.2	15.3	19.1	0.5	5.8	9.7	2.3	5.7	11.6	19.2
w^a	0.26	0.39	0.4	0.11	0.31	0.34	0.22	0.31	0.78	0.89
m	12	12	12	12	12	12	12	12	1	1
T_L	2.25	5.29	6.06	0.28	2.58	3.66	1.17	2.55	2.66	3.90
$\ln k$	-7.3	-70.4	-79.3	26.3	-14.8	-34.9	6.3	-14.5	-12.7	-27.9

^a Calculated at half-height (half ΔE^\ddagger).

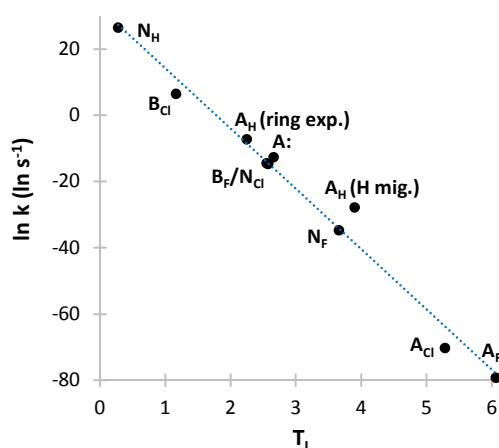


Figure 10 Tunneling limit (eq. 3) vs. $\ln k$ at 10 K for all the reactions in this study (see Table 3).

Conclusions

In this work we studied the heavy atom tunneling possibility at cryogenic temperatures for the carbene-based ring expansion of adamantane, noradamantane and bisnoradamantane to produce homoadamantene, adamantene and noradamantene (with the strain and reactivity of the partaking C-C bond growing in that order). To experimentally detect the decaying carbene, its reactivity has to be modulated with the stabilization granted by the second substituent: a hydrogen, chlorine or fluorine. The strong electron donation from a p AO of F on the empty p AO of the carbene stabilizes the system, making the fluorine complementary to the most reactive bisnoradamantane, and producing a carbene with a predicted observable lifetime (**B_F**). Cl, less prone to the stabilization by charge transfer, works well with the noradamantyl system (**N_{Cl}**).^{16,17} Finally H, completely lacking p orbitals to stabilize the carbene, will match the less reactive adamantane (**A_H**).

Although the barrier height is an intrinsically important factor for the tunneling rate, more decisive is the barrier width. Nevertheless these two variables are connected, and for similar systems a lower activation energy generally produces a narrower crossing (a corollary of the Hammond postulate). Therefore, the described reactions that occur exclusively by tunneling have similar ΔE^\ddagger of circa 6 kcal/mol, producing half-height barrier width of approximately 0.3 Å for the carbene displacement.

N_{Cl} has been proven experimentally¹⁶ and theoretically¹⁷ to have the “right” lifetime to be detected during the tunneling process. **B_F** has a very similar computed rate constant, and therefore the same behaviour is predicted.

Since in the **A_H** system the barrier is narrower (0.26 Å for the carbene half-height barrier width), the reaction is significantly faster than for the noradamantyl and bisnoradamantyl cases, and the carbene will be much harder (but not impossible) to detect experimentally,²⁰ even though its ΔE^\ddagger is slightly higher than in the **N_{Cl}** and **B_F** cases.

An atomic displacement and KIE analysis shows that the carbene is the tunneling determining atom (TDA) in the QMT mechanism at cryogenic temperatures, but other carbons can also affect the rate. The mass of the Cl and F substituents produces small but non-negligible effect on the tunneling. There is an unexpected boost on the rate of adamantyl-carbene when the H is substituted by a D, caused by an inverted secondary KIE; this enhances the classical (CVT) rate with a higher substituent mass, overcoming the countering QMT effect.

In an effort to compare the requirements of carbon vs. hydrogen tunneling, an H-shift on adamantylidene was studied. The experimental values³⁹ and the theoretical results presented here show that this system, which has a resemblance to the previously studied ones, also occurs by QMT with an “experimentally observable” lifetime. The comparison of these reactions revealed that to obtain similar rates, a carbon migration must have a barrier of approximately half the height and a third of the width of a hydrogen migration.

Finally, a tunneling limit (T_L) condition is proposed, which can serve as a fast, qualitative test to see if a reaction has a chance of happening by QMT.

Acknowledgements

The author wish to thank the fruitful insights provided by Weston T. Borden, the abundant technical support of David A. Hrovat and the advices and corrections of Mariela Pavan.

Notes and references

^a Department of Chemistry and Center for Advanced Scientific Computing and Modeling (CASCaM), University of North Texas, Denton, TX 76201, USA.

E-Mail: seb.kozuch@gmail.com

[†] Formally speaking, the activation energy is an empirical parameter estimated from the rate constant as $E_a = -RT^2 \cdot [d \ln k / dT]$.⁴² By mixing this expression with the transition state theory it can be derived that $E_a = \Delta H^\ddagger + RT$. In this manuscript we will use ΔE^\ddagger , the energy difference between the TS and the intermediate, as the definition of energy of activation or energy barrier. This is simpler to compute, and at the same time it is analogous to other activation definitions, such as ΔH^\ddagger and ΔG^\ddagger .

[§] The possibility of rearrangement of excited diazo and diazirine precursors or the inefficient quenching in the Ar matrix of excited states after the photolysis may limit the experimental observation of highly reactive singlet carbenes. The appearance of triplet carbenes can also change the rules of the game, but this does not seem to be the case of the systems studied here. CCSD(T)-F12/vdz-f12//B3LYP/6-31g(d) calculations on **N_H** indicates that the singlet is 2.9 kcal/mol more stable than the triplet, while previous calculations on **N_{Cl}** put the singlet-triplet excitation in 2.0 kcal/mol.¹⁷

Electronic Supplementary Information (ESI) available: XYZ geometries and rates of reactions at different temperatures. See DOI: 10.1039/b000000x/

1. R. P. Bell, *The tunnel effect in chemistry*, Chapman and Hall, London; New York, 1980.
2. J. Kästner, *WIREs Comput. Mol. Sci.*, 2013, **Early View**, DOI: 10.1002/wcms.1165.
3. J. Kästner, *Chem. Eur. J.*, 2013, **19**, 8207–8212.
4. D. W. Whitman and B. K. Carpenter, *J. Am. Chem. Soc.*, 1980, **102**, 4272–4274.
5. D. W. Whitman and B. K. Carpenter, *J. Am. Chem. Soc.*, 1982, **104**, 6473–6474.
6. B. K. Carpenter, *J. Am. Chem. Soc.*, 1983, **105**, 1700–1701.
7. P. S. Zuev, R. S. Sheridan, T. V. Albu, D. G. Truhlar, D. A. Hrovat, and W. T. Borden, *Science*, 2003, **299**, 867–870.
8. D. Gerbig, D. Ley, and P. R. Schreiner, *Org. Lett.*, 2011, **13**, 3526–3529.
9. A. Datta, D. A. Hrovat, and W. T. Borden, *J. Am. Chem. Soc.*, 2008, **130**, 6684–6685.
10. O. M. Gonzalez-James, X. Zhang, A. Datta, D. A. Hrovat, W. T. Borden, and D. A. Singleton, *J. Am. Chem. Soc.*, 2010, **132**, 12548–12549.
11. X. Zhang, D. A. Hrovat, and W. T. Borden, *Org. Lett.*, 2010, **12**, 2798–2801.
12. H. Inui, K. Sawada, S. Oishi, K. Ushida, and R. J. McMahon, *J. Am. Chem. Soc.*, 2013, **135**, 10246–10249.
13. S. L. Buchwalter and G. L. Closs, *J. Am. Chem. Soc.*, 1975, **97**, 3857–3858.
14. S. L. Buchwalter and G. L. Closs, *J. Am. Chem. Soc.*, 1979, **101**, 4688–4694.
15. E. M. Greer, C. V. Cosgriff, and C. E. Doubleday, *J. Am. Chem. Soc.*, 2013, **135**, 10194–10197.
16. R. A. Moss, R. R. Sauers, R. S. Sheridan, J. Tian, and P. S. Zuev, *J. Am. Chem. Soc.*, 2004, **126**, 10196–10197.

17. S. Kozuch, X. Zhang, D. A. Hrovat, and W. T. Borden, *J. Am. Chem. Soc.*, 2013, **135**, 17274–17277.
18. R. A. Moss, *Acc. Chem. Res.*, 2006, **39**, 267–272.
19. R. A. Moss and M. E. Fantina, *J. Am. Chem. Soc.*, 1978, **100**, 6788–6790.
20. E. L. Tae, C. Ventre, Z. Zhu, I. Likhovtorik, F. Ford, E. Tippmann, and M. S. Platz, *J. Phys. Chem. A*, 2001, **105**, 10146–10154.
21. E. L. Tae, Z. Zhu, and M. S. Platz, *J. Phys. Chem. A*, 2001, **105**, 3803–3807.
22. G. Yao, P. Rempala, C. Bashore, and R. S. Sheridan, *Tetrahedron Lett.*, 1999, **40**, 17–20.
23. D. Ley, D. Gerbig, and P. R. Schreiner, *Org. Biomol. Chem.*, 2012, **10**, 3781.
24. D. Ley, D. Gerbig, and P. R. Schreiner, *Chem. Sci.*, 2013, **4**, 677–684.
25. B. C. Garrett and D. G. Truhlar, *J. Chem. Phys.*, 1983, **79**, 4931.
26. A. Fernandez-Ramos, B. A. Ellingson, B. C. Garrett, and D. G. Truhlar, in *Rev. Comput. Chem.*, eds. K. B. Lipkowitz and T. R. Cundari, John Wiley & Sons, Inc., 2007, vol. 3, pp. 125–232.
27. A. D. Becke, *J. Chem. Phys.*, 1993, **98**, 5648.
28. P. J. Stephens, F. J. Devlin, C. F. Chabalowski, and M. J. Frisch, *J. Phys. Chem.*, 1994, **98**, 11623–11627.
29. P. C. Hariharan and J. A. Pople, *Theor. Chim. Acta*, 1973, **28**, 213–222.
30. J. Zheng, Y. Zhao, and D. G. Truhlar, *J. Chem. Theory Comput.*, 2009, **5**, 808–821.
31. *Gaussian 09, Revision C.01*, M. J. Frisch, G. W. Trucks, H. B. Schlegel, G. E. Scuseria, M. A. Robb, J. R. Cheeseman, G. Scalmani, V. Barone, B. Mennucci, G. A. Petersson, H. Nakatsuji, M. Caricato, X. Li, H. P. Hratchian, A. F. Izmaylov, J. Bloino, G. Zheng, J. L. Sonnenberg, M. Hada, M. Ehara, K. Toyota, R. Fukuda, J. Hasegawa, M. Ishida, T. Nakajima, Y. Honda, O. Kitao, H. Nakai, T. Vreven, J. A. Montgomery, Jr., J. E. Peralta, F. Ogliaro, M. Bearpark, J. J. Heyd, E. Brothers, K. N. Kudin, V. N. Staroverov, R. Kobayashi, J. Normand, K. Raghavachari, A. Rendell, J. C. Burant, S. S. Iyengar, J. Tomasi, M. Cossi, N. Rega, J. M. Millam, M. Klene, J. E. Knox, J. B. Cross, V. Bakken, C. Adamo, J. Jaramillo, R. Gomperts, R. E. Stratmann, O. Yazyev, A. J. Austin, R. Cammi, C. Pomelli, J. W. Ochterski, R. L. Martin, K. Morokuma, V. G. Zakrzewski, G. A. Voth, P. Salvador, J. J. Dannenberg, S. Dapprich, A. D. Daniels, Ö. Farkas, J. B. Foresman, J. V. Ortiz, J. Cioslowski, and D. J. Fox, *Gaussian, Inc.*, Wallingford CT, 2009.
32. J. Zheng, S. Zhang, B. J. Lynch, J. C. Corchado, Y.-Y. Chuang, P. L. Fast, W.-P. Hu, Y.-P. Liu, G. C. Lynch, K. A. Nguyen, C. F. Jackels, A. Fernandez Ramos, B. A. Ellingson, V. S. Melissas, J. Villà, I. Rossi, E. L. Coitiño, J. Pu, T. V. Albu, R. Steckler, B. C. Garrett, A. D. Isaacson, and D. G. Truhlar, *POLYRATE 2010-A: Computer Program for the Calculation of Chemical Reaction Rates for Polyatomics.*, .
33. J. Zheng, S. Zhang, J. C. Corchado, Y.-Y. Chuang, B. A. Ellingson, E. L. Coitiño, and D. G. Truhlar, *GAUSSRATE 2009-A*, .
34. D. G. Truhlar and B. C. Garrett, *Annu. Rev. Phys. Chem.*, 1984, **35**, 159–189.
35. J. G. Lauderdale and D. G. Truhlar, *Surf. Sci.*, 1985, **164**, 558–588.
36. D. Gerbig and D. Ley, *WIREs Comput. Mol. Sci.*, 2013, **3**, 242–272.
37. T. Bally, S. Matzinger, L. Truttman, M. S. Platz, and S. Morgan, *Angew. Chem. Int. Ed.*, 1994, **33**, 1964–1966.
38. A. C. Udding, J. Strating, H. Wynberg, and J. L. M. A. Schlatmann, *Chem. Commun.*, 1966, 657.
39. D. Krois, L. Brecker, A. Werner, and U. H. Brinker, *Adv. Synth. Catal.*, 2004, **346**, 1367–1374.
40. W. Knoll, D. Kaneno, M. M. Bobek, L. Brecker, M. G. Rosenberg, S. Tomoda, and U. H. Brinker, *J. Org. Chem.*, 2012, **77**, 1340–1360.
41. V. C. Rojisha, K. Nijesh, S. De, and P. Parameswaran, *Chem. Commun.*, 2013, **49**, 8465–8467.
42. IUPAC Gold Book <http://goldbook.iupac.org>.